Experimental Investigation of a Vapor-injected Reciprocating Compressor for Use in a Multi-Evaporator Domestic Refrigerator/Freezer

Changkuan LIANG*, Daniel A. BENADOF, Haotian LIU, James E. BRAUN, Eckhard A. GROLL, Davide ZIVIANI

Ray W. Herrick Laboratories, Purdue University Mechanical Engineering
West Lafayette, IN, USA
liang160@purdue.edu; dbenadof@purdue.edu; liu1460@purdue.edu; jbraun@purdue.edu; groll@purdue.edu; dziviani@purdue.edu

*Corresponding Author

ABSTRACT

Domestic refrigerators account for approximately 4% of all energy consumed worldwide and mainly rely on vapor compression cycles to operate. To enable smarter, more versatile, and more energy efficient systems, advanced cycle architectures are of interest. In our previous work, a multi-evaporator vapor-injected cycle architecture has been investigated, and initial assessments estimated nearly 13% reduction in power consumption compared to a baseline existing system. Then, a mechanistic vapor-injected reciprocating compressor model was developed to investigate the design trade-offs and injection location and timing. Modeling results showed up to 10.7% decrease in specific work required and a parametric study revealed the importance of injection timing on the compressor efficiency. The current paper describes the design and initial test results for a prototype of the vapor-injected reciprocating compressor. A fast-acting solenoid and in-line check valve are connected and mounted directly on the cylinder wall to reduce dead volume during compression. The solenoid valve is controlled using the crank angle measurement from a Hall-effect sensor detecting a series of specifically placed magnets on the crankshaft. The prototype compressor was tested using a hot-gas-bypass compressor test stand under different suction, discharge and injection pressures. The experimental results show the prototype compressor's specific work was reduced by up to 25% during vapor-injected operation compared to its single-stage operation with no injection. The results also showed the specific work reduction increased with an increase of injection pressure when condensing and suction pressures were fixed.

1. INTRODUCTION

Domestic refrigerators/freezers are essential appliances in modern households and contribute to a significant amount of energy consumption around the world. In fact, the IIR (International Institute of Refrigeration) estimates 2 billion units are currently in operation and consume 4% of global electricity (IIR, 2019). This high energy consumption is due not only to the large number of devices in operation, but also to their average low thermodynamic efficiency (around 15% of Carnot COP) (Hermes & Melo, 2008). To reduce the energy consumption of these systems, advanced cycle architectures such as multi-stage vapor-injected cycle were considered in previous studies (Choi et al., 2018). For instance, Liang et al. (2022) investigated a triple-evaporator bypass circuit domestic refrigerator/freezer as a baseline system. The baseline system is state-of-the-art in its class that allows control of individual compartment temperatures with improved overall energy efficiency. The authors evaluated a two-stage vapor-injected cycle modification to this baseline that could improve overall energy performance while maintaining capacity and controllability. This cycle could establish two distinct evaporation temperatures for the refrigerator and freezer cabinets. This could effectively reduce the temperature difference between the refrigerator cabinet and its evaporator and thus reduce the heat transfer irreversibilities. By modifying a validated dynamic model of the baseline system, a two-stage vapor-injection cycle was analyzed in the previous work and the average power consumption of the modified system was reduced by up to 12.9% when compared to the baseline while maintaining the same temperature set points in all the cabinets

The previous study (Liang et al., 2022) used a simplified efficiency-based compressor model for both low and high stage compressors with a mixing section in between as shown in **Figure 1**. In order to understand the full benefits of

the proposed cycle, it is very important to accurately predict the vapor-injected compressor performance. A mechanistic vapor-injected reciprocating compressor model employing R600a as the working fluid was developed to be coupled with the established model for the modified multi-stage vapor injection cycle for a domestic refrigerator/freezer by Liang et al. (2023). It was assumed that the vapor-injected mass flow is controlled and separated from the suction flow by a fast-acting solenoid valve. It was identified that injection opening time of the injection flow is a key factor for overall compressor performance. The model predicted that the compressor's specific work would be reduced by 10.7% when compared to the baseline compressor.

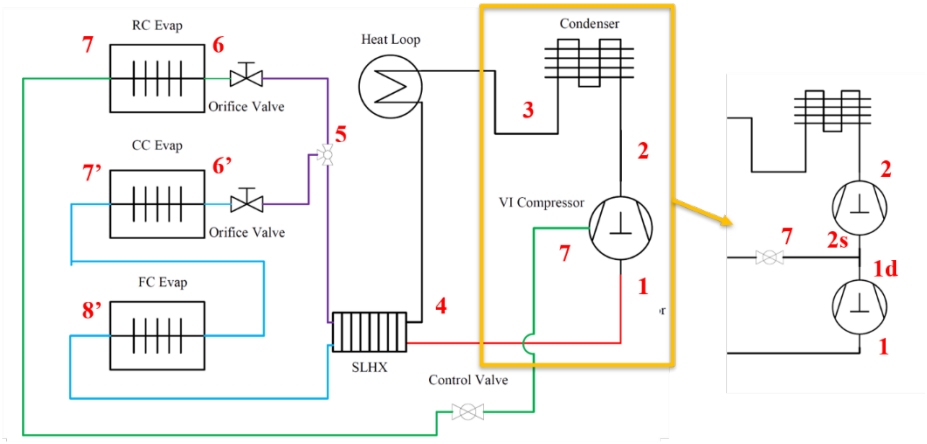

Figure 1. Schematic of the modified multi-stage vapor-injected cycle used in Liang et al. (2022)

In the current work described in this paper, a prototype vapor-injected reciprocating compressor was designed, assembled and tested. The prototype compressor was developed by modifying an existing R600a fixed-speed reciprocating compressor. A fast-acting solenoid and check valve were mounted together directly on the cylinder head to minimize dead volume during compression. The solenoid valve was controlled using the crank angle measurement from a Hall-effect sensor detecting a series of specifically placed magnets on the crankshaft. The prototype compressor was tested on a hot-gas-bypass compressor test stand under different suction, discharge and injection pressures to evaluate its performance.

2. VAPOR-INJECTION IN RECIPROCATING COMPRESSORS

To prototype a vapor-injected reciprocating compressor, it is important to understand the dynamics associated with both compression and vapor injection processes. In a typical suction stroke of a reciprocating compressor, the inside cylinder pressure is lower than the suction pressure to allow a reed valve to open due to a pressure difference. During the suction process, the piston reaches bottom dead center (BDC) when it is closest to the crankshaft. The piston then moves towards top dead center (TDC) and the volume of the compression chamber decreases and the pressure inside the cylinder increases. For vapor injection with multi-stage operation, the injection should occur at a point in the compression stroke where the intermediate injection pressure is close to, but greater than the cylinder pressure. As explained in Liang et al. (2023), for a reciprocating compressor, when the piston is at BDC, all the area is open to the chamber and an open injection port would continuously mix injection flow and suction flow until the cylinder pressure reached the intermediate pressure and then there would back flow. For a vapor-injected reciprocating compressor, a fact-responding control valve is necessary in the injection line as shown in **Figure 2** to control the timing and duration of refrigerant injection. In this work, a fast-acting solenoid valve controlled by an electronic signal based on the angle of the crankshaft is used. An additional check valve is also placed in the injection line to prevent any backflow through the line if cylinder pressure is greater than the intermediate pressure.

It should be noted that the main benefit of using a vapor-injected reciprocating compressor is the reduction of the specific work required. The specific work required is the amount of work required per unit mass flow. In terms of isentropic efficiency, the vapor injection process reduces both the isentropic and actual work. The reduction of the work comes from the cooling effect of the injected refrigerant. This increases the density of the refrigerant entering the second stage compression and reduces the specific work required. When applied in a refrigeration system, the injection line refrigerant comes from a medium-temperature evaporator while the suction line refrigerant comes from

low-temperature evaporator. This allows the cycle to establish two distinct evaporation temperatures for the refrigerator and freezer cabinets and effectively reduce the temperature difference between the refrigerator cabinet and its evaporator and thus reduce the heat transfer irreversibilities. The vapor-injected reciprocating compressor is key in realizing the energy reduction potential of a two-stage vapor-injected domestic refrigerator/freezer.

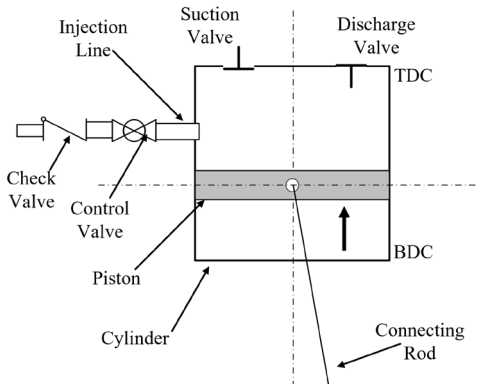

Figure 2. Illustration of the compression cylinder for the vapor-injected reciprocating compressor

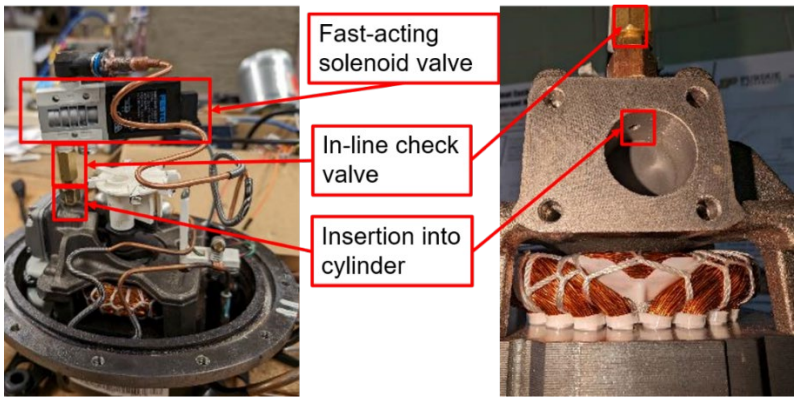

Figure 3 Prototype compressor fact-acting solenoid valve and check valve installation on compressor cylinder

3. PROTOTYPE COMPRESSOR DESIGN AND INSTRUMENTATION

In this study, the prototype vapor-injected reciprocating compressor was developed by modifying an Embraco EMD55CLT fixed-speed reciprocating compressor employing R600a as the refrigerant. The baseline compressor has a displacement volume of 9.04cc and a compressor speed of 60Hz. The modifications and additional components were selected based on both their functionality and cost. As the cost of the current reciprocating compressor used in domestic refrigerator/freezer application is quite low, the prototype compressor did not use overly expensive components or methods to remain realistic in potential market application.

3.1 Injection Port and Check Valve

The vapor-injected reciprocating compressor requires a fast-acting solenoid valve. For this study, the Festo MHE3-MS1H-3/2G-1/8 three-port two-position air solenoid valve with 1/8-inch (3.2 mm) pneumatic connection was used. As the injected refrigerant is superheated vapor, the air solenoid valve is deemed an appropriate choice. This valve is a pressure-relieved poppet valve with mechanical spring for reset. Its maximum switching frequency is 280Hz. The switch-on time is 2.3 ms and the switch-off time is 2.8 ms. Since the compressor's operation speed is 60Hz, the solenoid valve's switching frequency is considered to be fast enough. In addition, the switch-on time can be accounted for during the compressor's operation by sending the opening signal at an earlier crank angle.

A H-1/8-A/I Festo in-line non-return valve was connected between the solenoid valve and the compressor cylinder to avoid backflow during the compression process. The valve arrangement can be seen in **Figure 3**. The check valve was

connected to one of the ports on the solenoid valve on one end and connected through a custom-made fitting to an opening on the compressor cylinder on the other end. This opening was 1/8 inch (3.2mm) in diameter serving as an injection port. This injection port was placed 10 mm from the top of the compression cylinder. It was chosen for its relative ease of access when installing the fitting to create the opening on the compression cylinder. In addition, at this injection location, the injection area would stay covered by the piston once it moves past the injection area in the compression stroke. The injection refrigerant then cannot be exposed to the shell and leak out due to pressure difference. While this issue can also be solved by closing the solenoid valve when the piston moves past the injection area, it is more demanding on the solenoid valve control as the opening and closing time can be very close.

3.2 Crank Angle Measurement

An A3144 Hall-effect sensor was used to measure the crank angle of the compressor during each revolution. A trigger wheel was designed to be fitted on top of the crank shaft and hold the magnets for the sensor at certain intervals. It was designed to fit on the counterweight and crankshaft pin on top of the crank shaft, as seen in **Figure 4** on the right. The trigger wheel in this study was 3D-printed with ABS plastic. It is very light and causes minimal additional vibration when attached to the crank shaft on the counterweight. The trigger wheel has seven spokes, each 45 degrees apart. A missing spoke corresponds to the TDC during compressor operation and is used to index the revolution. Considering the radius of the trigger wheel must be smaller than the compressor shell, 45 degrees between each spoke was selected to ensure enough distance for the Hall-effect sensor to accurately produce a digital signal.

Figure 5 illustrates the trigger wheel and the Hall-effect sensor installation on the compressor. The Hall-effect sensor was mounted on a 3D printed sensor stand such that it was within its detection range with respect to the trigger wheel. The sensor stand was directly mounted on the compressor block to ensure its stability during operation.

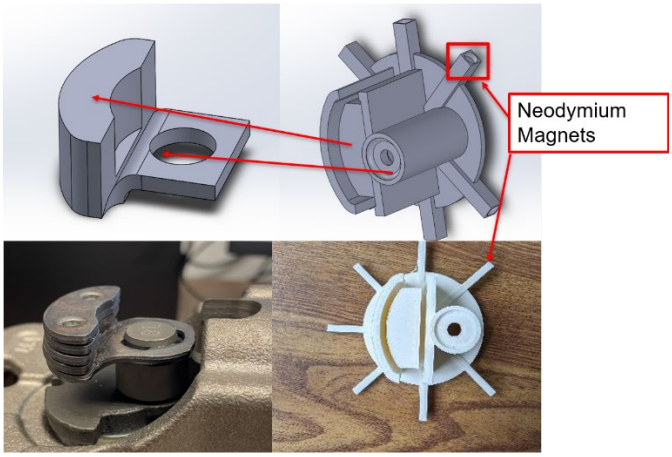

Figure 4 Prototype compressor trigger wheel design

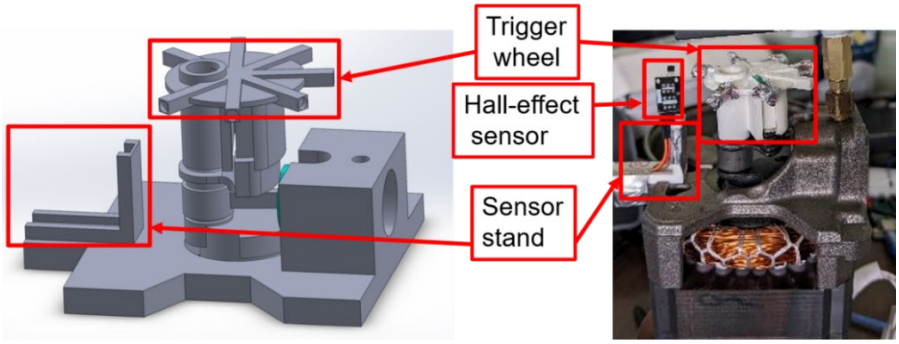

Figure 5 Prototype compressor trigger wheel and Hall-effect sensor installation

3.3 Compressor Controller and Shell

An Arduino Uno microcontroller was used in the prototype compressor to control the opening of the injection valve. The microcontroller has a 16MHz ceramic resonator as its internal clock. During operation, the sampling speed was kept at 1MHz, or once every microsecond. The controller reads the digital signal from the Hall-effect sensor and calculates the current crank angle during the compression cycle based on the amount of time passed since the last time the controller receives a signal from the Hall-effect sensor. At the desired injection radian, the controller sends a digital signal to a PN2222 NPN transistor to switch on the solenoid valve.

The prototype compressor used a custom-made semi-hermetic shell for enabling access to components, such as the solenoid valve and Hall-effect sensor, when necessary. The prototype compressor's shell design can be seen in **Figure 6**. To produce this custom-made shell, the original hermetic shell was cut in half. The top half was then welded to a cast iron sheet to extend the space inside the shell in order to accommodate the additional components. A 1/4 inch (6.35 mm) metal flange was then welded on both the top and bottom half of the shell to securely connect both shells. To seal the compressor, a groove was made inside the metal flange with a special O-ring fit into the groove. A 1/4 inch (6.35 mm) diameter NPT female connection was made on the top shell to fit a hermetic feedthrough fitting that carries 12 wires. This feedthrough was used to carry the electronic signal used for the controller to read the Hall-effect sensor and open the solenoid valve. The compressor was pressure tested with dry nitrogen up to 250 psi (1723 kPa) without any leakage.

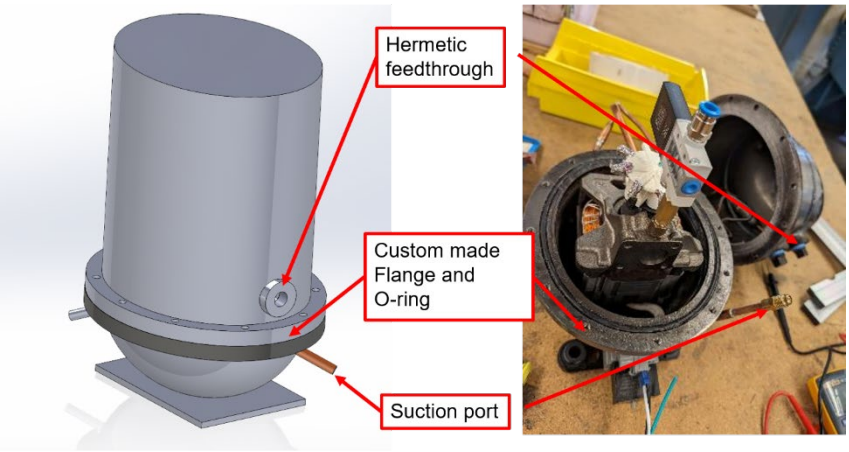

Figure 6 Custom-made compressor shell design

3.4 Hot-gas-bypass Test Stand and Instrumentation

The prototype compressor was tested on a hot-gas-bypass test stand modified for vapor-injected compressors. **Figure 7(a)** shows a schematic for the test stand and **Figure 7(b)** illustrates the hot-gas-bypass cycle on a P-h diagram. The hot-gas-bypass cycle splits a portion of high-enthalpy refrigerant before it enters the condenser (state 3) and is expanded to lower pressures (states 5 and 7). The bypassed refrigerant that is expanded to suction pressure (state 5) is mixed with expanded refrigerant from the condenser outlet (state 6) and the mixture flows to the compressor inlet (state 1). The bypassed refrigerant that is expanded to an intermediate pressure (state 7) is also mixed with expanded refrigerant from the condenser (state 8) and the mixture serves as the compressor's injection gas (state 9). Through adjusting the expansion valves for both the bypass and condenser outlet refrigerant, the temperature and pressure of the suction and injection gas can be controlled to a desired level. This test stand allows the compressor's performance to be tested at various operating conditions without sizing and installing different heat exchangers. **Figure 7(c)** shows the test stand with the prototype vapor-injected reciprocating compressor installed.

On this test stand, a total of 12 T-type thermocouples were installed (not all shown on the schematic) to measure temperatures at the inlets and outlet of the compressor as well as various points across the cycle. Four pressure transducers were installed to measure the suction, discharge and injection pressure of the compressor as well as the intermediate pressure of the hot-gas-bypass cycle. Two mass flow meters were installed in the test stand. One was installed at the test stand's suction line while the other one was installed at the discharge line after the oil separator.

The difference between these two measured mass flow rates should be the injection mass flow rate. A power meter was also installed to measure the real time power consumption of the compressor. The specifications of all the instruments can be found in **Table 1**. The data acquisition system used in this study was an Agilent Technology 34980A.

Table 1 Measuring instrumentation specifications

Description	Name	Range	Uncertainty
Thermocouple	T-type	-250-350 ℃	± 0.5 ℃
Pressure transducer (high pressure)	Omega PX359	0 to 2068.43 kPa (300 psi)	±1%
Pressure transducer (low pressure)	Setra 206	0 to 344.74 kPa (50 psi)	±0.13 %
Mass flow meter (discharge)	Emerson micro motion CMFS010	0 to 110 kg/h	±0.25 %
Mass flow meter (suction)	Emerson micromotion CMFS007	0 to 40.9 kg/h	+0.25 %
Power meter	Scientific Columbus XL5C5PAN7	0 to 500 W	±0.2 %

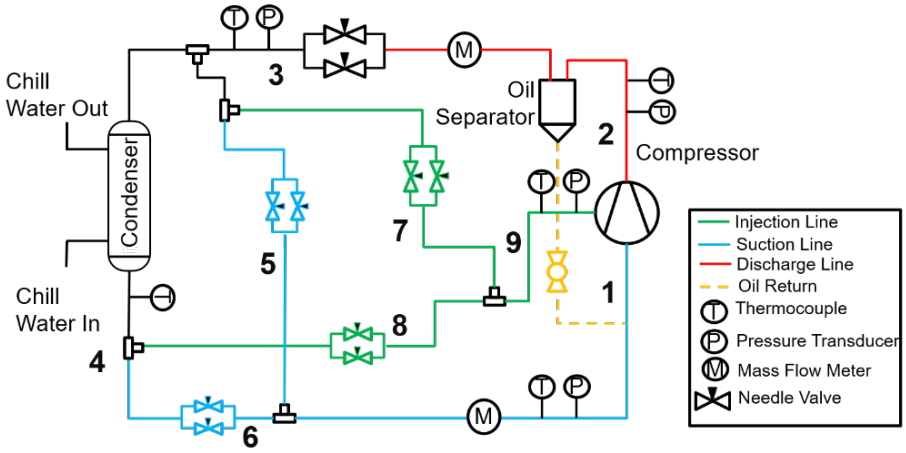

(a) Hot-gas-bypass test stand schematic

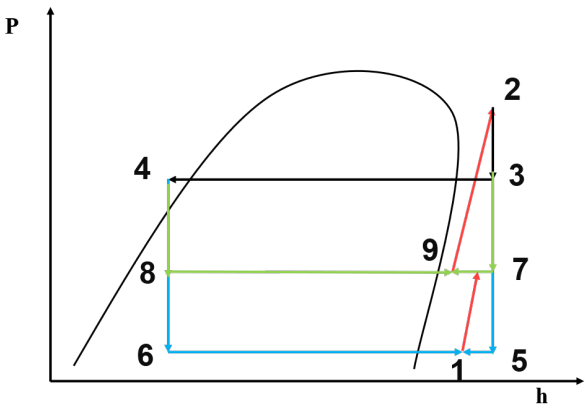

(b) P-h diagram of a hot-gas-bypass cycle for vapor-injected compressor

(c) Hot-gas-bypass test stand with prototype compressor installed

Figure 7 Hot-gas-bypass test stand schematic, P-h diagram, and picture

3.5 Isentropic and Volumetric Efficiency Calculation

In this study, isentropic efficiency is defined as the ratio of the measured compressor power consumption to the power consumption needed for a reversible and adiabatic (isentropic) process from suction to discharge pressure as presented in Bahman et al. (2018). The overall compression process isentropic efficiency is determined as:

$$\eta_{oa,isen} = \frac{\dot{m}_{suc}\left(h_{inj,isen} - h_{suc}\right) + \dot{m}_{tot}(h_{dis,isen} - h_{inj,isen,mix})}{\dot{W}_{comp}} \quad (1)$$

where $\dot{m}_{suc}$ and $\dot{m}_{tot}$ refer to suction and discharge mass flow rate. $h_{inj,isen}$ refers to the enthalpy at the pressure of the injection flow with the specific entropy at low stage suction. $h_{inj,isen,mix}$ refers to the mixture state that begins the second stage compression and is determined based on isentropic compression in the first stage and adiabatic mixing at the injection pressure according to Equation 2:

$$h_{inj,mix} = \frac{\dot{m}_{suc}h_{inj,is} + \dot{m}_{inj}h_{inj}}{\dot{m}_{tot}} \quad (2)$$

It is then used to calculate the $h_{dis,isen}$, the enthalpy of the refrigerant at discharge pressure after isentropic compression.

Volumetric efficiency is defined as the ratio of the measured suction mass flow rate to the theoretical maximum compressor suction mass flow rate, determined using the following equation:

$$\eta_{vol} = \frac{\dot{m}_{suc}}{\rho_{suc}V_{disp}N_c} \quad (3)$$

where ρ_{suc} is the density of the suction gas, V_{disp} is the compression displacement volume and N_c is the compressor frequency.

4. RESULTS AND DISCUSSION

For this study, the compressor ran at 60Hz while the injection timing was fixed at 250 degrees during the compression process (TDC is considered to be 0 degree) for all the conditions. Data presented in this section were obtained with at least 10 minutes of steady-state operation in which all the pressure measurements remained within ± 5 kpa. Further, the suction and injection temperatures were kept at 24 ℃ during the experiments for all conditions.

Table 2 shows a comparison between the prototype compressor's single-stage operation and vapor-injected operation at the same condition. For this comparison, the discharge pressure was kept at 290 kPa while the suction pressure was kept at 65 kPa. The injection pressure during vapor-injection operation was kept at 95 kPa. This condition was chosen for demonstrating the compressor's performance in vapor-injection mode. From the table, it can be seen that during vapor-injected operation the injection mass flow rate was 0.09 g/s, which was 56.7% of the suction mass flow. The power consumption during vapor-injected operation was 4.46% more than that during single-stage operation. Further, vapor-injected operation decreased the discharge temperature by 0.84 ℃ and increased the isentropic efficiency by 42.8%. The volumetric efficiency stayed the same since the compressor inlet conditions were the same in both cases leading to the same mass flow rate. The specific work required for the compressor was reduced by 25%. As discussed in Section 2, this reduction in required specific work is the main benefit for the vapor-injected compressor.

It should be noted that the isentropic efficiency, volumetric efficiency and mass flow rates were lower than expected compared to the manufacturer's compressor map, even for single-stage operation. The combination of the low volumetric and isentropic efficiency indicates that refrigerant is leaking from high pressure to low pressure somewhere within the compressor. This leakage could be from the injection line through fitting into the shell, across the piston, or across one or both valves that could have resulted from inadequate lubrication or damage during the compressor modifications. These possibilities will be investigated further in future work on the prototype compressor's performance. However, it is clear that the refrigerant injection had a significant impact on compressor performance, increasing discharge mass flow rate, power consumption, and isentropic efficiency while decreasing discharge temperature and specific work.

Table 2 Performance comparison between prototype compressor's single-stage and vapor-injected operation when $P_{discharge} = 290\ kPa, P_{suction} = 65\ kPa$ and $P_{injection} = 95\ kPa$

	Vapor-injected	Single-stage
Total mass flow (g/s)	0.24	0.15
Suction mass flow (g/s)	0.15	0.15
Injection mass flow (g/s)	0.09	N/A
Power consumption (W)	77.57	74.26
Discharge temperature (℃)	49.30	50.14
Specific work (J/g)	328.79	438.60
Isentropic Efficiency (-)	0.183	0.129
Volumetric Efficiency (-)	0.195	0.195

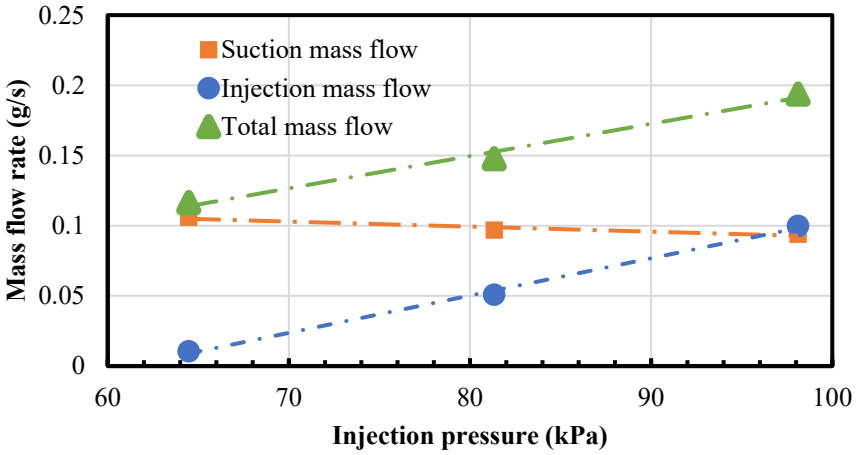

Figure 8 Prototype compressor's mass flow rates at different injection pressures when $P_{discharge} = 290$ kPa and $P_{suction} = 50$ kPa

Figure 8 shows the prototype compressor's mass flow rates at different injection pressures while the discharge and suction pressures were fixed at 290 kPa and 50 kPa. It can be seen that as the difference between the injection pressure and the suction pressure increased, the injection and total mass flow rates also increased. This is due to the fact that the injection mass flow is a pressure driven flow. At the moment the solenoid valve opens during the compression stroke, refrigerant in the injection line is driven by the pressure difference between the injection line and the compression cylinder. For specified suction and discharge pressures, the pressure inside the compression cylinder is uniquely dependent on the injection crank angle. This means if the injection pressure is larger, the pressure difference that drives the injection flow is also larger. Further, as seen in the figure, the injection pressure's effect on suction mass flow rate was minimal. During the compression process, the suction flow is driven by the pressure difference between the shell and compression cylinder's pressure at BDC. The compressor's suction pressure and mass flow rate should not be affected by the injection line. However, if the injection line fittings leak, then injection line refrigerant can leak into the shell and cause the suction mass flow rate to decrease by the amount leaked into the shell. The experimental result indicates that the prototype compressor's injection line did not leak since there was no effect of increased injection pressure on the suction mass flow rate.

Figure 9 shows the prototype compressor's power consumption and specific work at different injection pressures for fixed discharge and suction pressures of 290 kPa and 50 kPa. As seen in the figure, as the injection pressure increases, the power consumption also increases due to the additional injection mass flow rate. On the other hand, the specific work required decreases with the increased injection mass flow rate. This is due to the refrigerant entering high-stage compression having a higher density as a result of the increased injection mass flow rate and its cooling effect on the compression process. The trends exhibited by the prototype compressor's power consumption and specific work were expected. **Figure 10** shows the prototype compressor's isentropic efficiency at different injection pressures. From the

figure, the isentropic efficiency when injection pressure was at 81.33 kPa was lower than that at both higher and lower pressures. Further, the power consumption at this condition, shown in **Figure 9**, was particularly high. This could be due to measurement error and requires further investigation in future studies. However, this plot shows that in general, the isentropic efficiency of the prototype compressor increases with injection pressure as expected.

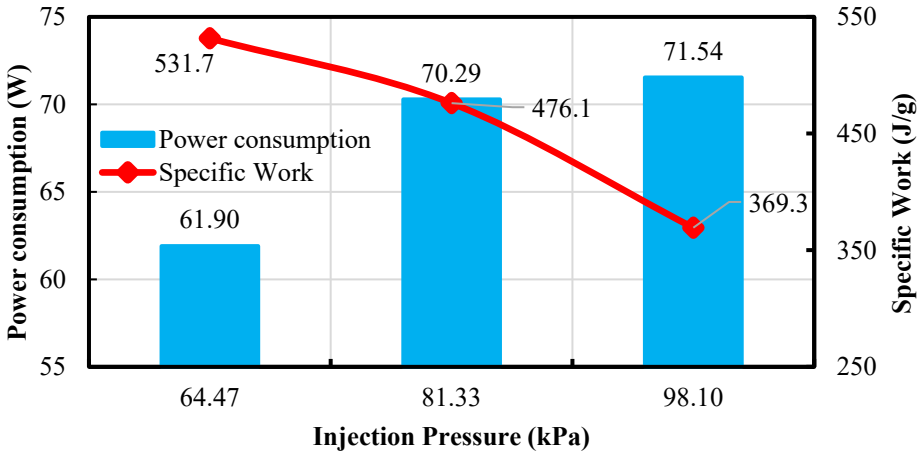

Figure 9 Prototype compressor's power consumption and specific work at different injection pressures when $P_{discharge} = 290\ kPa$ and $P_{suction} = 50\ kPa$

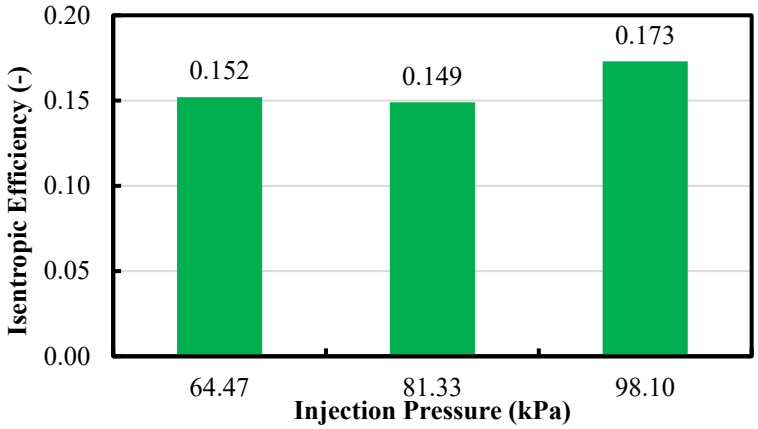

Figure 10 Prototype compressor's power consumption and specific work at different injection pressures when $P_{discharge} = 290\ kPa$ and $P_{suction} = 50\ kPa$

The results shown in this section demonstrated that the performance of the reciprocating compressor could be significantly improved through refrigerant injection. The prototype compressor's manufacturing method and material used readily available and low-cost technology to remain realistic in potential market application. For instance, the Hall-effect sensor (~$1) crank angle measurement technique is widely applied in the automotive industry. The trigger wheel (3D printed) for holding the magnet was necessary in this prototype but the counterweight on which the trigger wheel stands can be easily adjusted during the manufacturing process such that it can securely hold a magnet and still be able to counter the momentum from the piston during operation. The cast iron compressor block can be re-designed to secure the Hall-effect sensor. The fast-acting solenoid valve (~$170) was the most expensive component in the prototype compressor. However, this solenoid valve is very similar to a fuel injection valve in a modern internal combustion engine. The main difference is that a fuel injection valve is used for high-pressure liquid injection while the fact-acting solenoid valve is used for medium-pressure gas injection. But the fuel injection valve can be modified in terms valve opening area to ensure enough gas flow can be delivered at the desired temperature and pressure. The fuel injection valve's opening frequency and electronic connection is already suitable for the prototype compressor. Further, in this application, the fuel injection valve's atomization at the nozzle required for the high-pressure liquid is

not necessary for this application. A fuel injection valve is a relatively low-cost (~$40) and common item in the automotive market and repurposing it for the vapor-injection compressor can be easily done.

4. CONCLUSION

In this work, a prototype vapor-injected reciprocating compressor for use in a two-stage vapor-injected domestic refrigerator/freezer system was designed and assembled, and its performance tested. The prototype compressor was developed by modifying an existing R600a fixed-speed reciprocating compressor. A fast-acting solenoid and check valve were mounted together directly on the cylinder head to minimize dead volume during compression. The solenoid valve was controlled using the crank angle measurement from a Hall-effect sensor detecting a series of specifically placed magnets on the crankshaft. The prototype compressor was tested on a hot-gas-bypass compressor test stand under different suction, discharge and injection pressures to evaluate its performance. The experimental results show the prototype compressor's specific work was reduced by up to 25% for vapor-injected operation compared to single-stage operation with no injection. Through varying the injection pressure, the prototype compressor's injection and discharge mass flow rates, power consumption and specific work all showed expected results. The experimental results shown in this work demonstrate the prototype compressor was operating as designed.

Previous studies by the authors have shown the two-stage vapor-injected cycle can deliver 12.9% power consumption reduction for a modern flexible domestic refrigerator/freezer. The main difficulty in producing this system is the lack of a suitable compressor. This work presented a methodology for producing a vapor-injected reciprocating compressor suitable for domestic refrigerator/freezer application and proves the prototype compressor is operational. The experimental results showed that vapor-injection was able to reduce specific work required and increase isentropic efficiency. More importantly, the compressor can enable energy consumption reduction when implemented in a two-stage vapor-injected doemstic refrigerator/freezer system.

In terms of future work, the authors will investigate the effect injection timing has on the prototype compressor's performance. Further, a performance map will be developed for the prototype compressor across a range of suction, discharge and injection pressures as well as injection timing. These experimental results will be used to verify overall savings associated with application in a baseline refrigerator-freezer that were determined through modeling by Liang et al. (2023). Finally, an existing domestic refrigerator/freezer will be modified with a two-stage vapor-injected cycle utilizing the prototype compressor in order to further validate overall savings potential.

REFERENCES

Bahman, A., Ziviani, D., Groll, E. A. (2018). Vapor-injected compression with economizing in packaged air conditioning systems for high temperature climate. *International Journal of Refrigeration,* vol. 94, pp. 136-150.

Choi, S., Han, U., Cho, H., & Lee, H. (2018). Review: Recent advances in household refrigerator cycle technologies. In *Applied Thermal Engineering*, Vol. 132, pp. 560–574.

IIR. (2019). The role of refrigeration in global economy. *38th Informatory note of refrigeration technologies.*

Liang, C., Braun, J. E., Groll, E. A., Ziviani, D. (2022). Dynamic Modeling and Validation of a Triple-Evaporator Domestic Refrigerator/Freezer with R-600a. *19th International Refrigeration and Air Conditioning Conference at Purdue*. Paper 2501.

Liang, C., Liu, H., Ziviani, D., Braun, J. E., Groll, E. A. (2023). Numerical investigation of a vapor-injected reciprocating compressor for a multi-evaporator domestic refrigerator/freezer application. *13th International Conference on Compressors and Their Systems.* pp.369-381

ACKNOWLEDGEMENTS

The author would like to thank the faculty and staff and Ray W. Herrick Laboratories for all the technical support. Moreover, the author would also like to thank Whirlpool Corporation for technical support for this study.